coatings

MDPI

Article

Ball-Milling Preparation of La^{3+}/TiO_2 Photocatalyst and Application in Photodegradation of PVC Plastics

Yan Zhang [1,2], Tianyi Sun [1,2,*], Dashuai Zhang [1,2], Chen Li [1,2], Jinrui Liu [1,2], Bangsen Li [1,2] and Zaifeng Shi [1,2,*]

[1] Key Laboratory of Water Pollution Treatment & Resource Reuse, Hainan Normal University, Haikou 571158, China
[2] College of Chemistry and Chemical Engineering, Hainan Normal University, Haikou 571158, China
* Correspondence: tianyi870328@163.com (T.S.); zaifengshi@163.com (Z.S.)

Abstract: The fact that the use of a large number of plastic products has brought serious pollution to the environment has always been the focus of global attention. The development of photocatalytic degradable plastics is one of the effective ways to solve the problem of "white pollution". In this work, La^{3+} modified TiO_2 nanoparticles were prepared by ball milling and characterized. La^{3+}/TiO_2 was mixed with Polyvinyl chloride (PVC) plastic to make a photodegradable composite film, and the photodegradation performance and mechanical properties of films were evaluated. The photodegradable films were characterized by infrared spectroscopy (FT-IR), X-ray diffractometry (XRD), and scanning electron microscopy (SEM). After 30 h UV irradiation, the weight loss rate of the PVC was only 2.12%, while that of the TiO_2/PVC reached 8.94%. The accelerating of the degradation rate was due to the mixing of TiO_2 into PVC. As for the La^{3+}/TiO_2/PVC composite film, when the mass percentage of La^{3+}/TiO_2 was 1.5%, the weight loss rate of La^{3+}/TiO_2/PVC sample reached a maximum of 17.78%, which was eight times the degradation rate of PVC and two times the degradation rate of TiO_2/PVC. The La^{3+}/TiO_2/PVC film showed good photodegradability. La is a transition metal element with a special 4f electronic structure. The reaction mechanism of photodegradation of PVC by the interaction of La^{3+} and TiO_2 were discussed.

Keywords: La^{3+} modified TiO_2; La^{3+}/TiO_2/PVC composite film; ball milling method; photodegradation

check for updates

Citation: Zhang, Y.; Sun, T.; Zhang, D.; Li, C.; Liu, J.; Li, B.; Shi, Z. Ball-Milling Preparation of La^{3+}/TiO_2 Photocatalyst and Application in Photodegradation of PVC Plastics. *Coatings* **2023**, *13*, 317. https://doi.org/10.3390/coatings13020317

Academic Editor: Alexandru Enesca

Received: 9 December 2022
Revised: 26 January 2023
Accepted: 26 January 2023
Published: 31 January 2023

Copyright: © 2023 by the authors. Licensee MDPI, Basel, Switzerland. This article is an open access article distributed under the terms and conditions of the Creative Commons Attribution (CC BY) license (https://creativecommons.org/licenses/by/4.0/).

1. Introduction

PVC is one of the five biggest general-purpose plastics, having the characteristics of non-combustibility, corrosion resistance, chemical resistance, insulation, and good mechanical properties. Recently, PVC was widely used in industry, products, daily necessities, building materials, environmental protection materials, etc. [1,2]. However, with the increasing use of one-off plastic products, the pollution resulting from the plastic waste has become more and more serious [3,4]. Plastic pollution has always been a hot spot of global concern. The treatment methods are incineration, landfill [5], recycling, chemical degradation, and the production of degradable plastics [6,7]. Photodegradable plastics have been widely studied, which is an ideal way to solve the "white pollution" [8,9].

Photocatalysis is a green-friendly technology that combines abundant solar energy resources with environmental cleanup and resource reuse and has received widespread attention [10]. TiO_2, ZnO, CdS, and Fe_2O_3 are common semiconductor materials [11]. Because of its low cost, non-toxicity and its photocatalytic activity for the decomposition of various environmental pollutants, TiO_2 is widely used in the field of photodegradable plastics [12,13]. At the present stage, the main modification method of TiO_2 is to regulate the structure and composition of the catalyst, including the regulation of TiO_2 crystal structure and defects, grain size, and energy band position. TiO_2 can be doped with metal, non-metal, precious metal, and other elements, and can also be modified by surface photosensitization and semiconductor composite [14,15]. The modification of TiO_2 is aimed

at expanding the absorption range of TiO_2 to sunlight, promoting the efficiency of charge separation, inhibiting the recombination of photo-generated carriers and improving the stability of catalyst [16]. Rare earth is a type of transition metal element with a special 4f electronic structure. Lanthanum is second only to cerium in rare earth elements and is rich in resources. Therefore, rare earth doped modified TiO_2 has been widely studied to improve photocatalytic activity [17–20].

Due to its simple operation and low cost, the ball milling method is an effective method in the industry to efficiently mix solids and solid reactants by using the rotation or vibration of a ball mill [21]. The rare earth modified TiO_2 photocatalyst made by the ball milling method applied to the degradation of PVC waste plastic is of great significance for solving the problem of environmental pollution from the viewpoint of practical application.

In this paper, La^{3+}/TiO_2 photocatalyst was prepared by the ball milling method. The La^{3+}/TiO_2/PVC composite film was prepared by introducing La^{3+}/TiO_2 into PVC plastic. After being compared with the PVC and TiO_2/PVC films, the La^{3+}/TiO_2/PVC film was characterized and its photodegradability was also studied. Moreover, the reaction mechanisms of the photodegradation of PVC by the interaction of La^{3+} and TiO_2 were discussed.

2. Experimental

2.1. Materials

TiO_2 (Analytical reagent, the average particle size = 19.8 nm) was purchased from Komiou Chemical Reagent Co., Ltd., Tianjin, China. The PVC polymer was produced by Aladdin (K-Value: 62–60). La_2O_3 was provided by Hunan Rare Earth Metal Materials Research Institute. N,N-dimethylformamide (AR), abbreviated as DMF, was produced by the Damao Reagent Company, Tianjin, China. Hydrochloric acid (HCl, 36.0–38.0%) was provided by Fusheng Industry Co., Ltd., Shanghai, China.

2.2. Characterization

Using Shimadzu UV-2600 ultraviolet-visible diffuse reflectance instrument, with $BaSO_4$ as a reference, the ultraviolet-visible absorption spectrum of the films was measured. Under the condition of vacuum 5×10^{-4} Pa, a JEOL Ltd. JSM-7100F thermal field emission scanning electron microscope (SEM, Electronics Co., Ltd., Japan) was used to test the surface morphology of the films, and the voltage was 5.0 kV. The samples were characterized by Thermo Scientific Nicolet 6700 Fourier transform infrared spectroscopy (FT-IR, Thermo Fisher Instruments Co., Waltham, MA, USA). The crystal phase of the materials was detected on an X-ray diffractometer (XRD, Pruck instruments Co., Germany) with Cu/K radiation, and the diffraction intensity was recorded in the 2θ range of 10–80° at a scanning speed of 5°/min. The digital display tensile testing machine was used to test the mechanical properties of the film, and purchased from Guangdong Zhongye Jingke Instrument Equipment Co., Ltd., Guangdong, China. The film was cut into a rectangle of 50 mm × 10 mm and fixed on the digital tensile testing machine with an initial spacing of 20 mm, running at a 50 mm/min. The thickness of the film was measured 5 times with the NSCING electronic digital micrometer, and the average value was taken.

2.3. Preparation of the La^{3+}/TiO_2 Photocatalyst

The La^{3+}/TiO_2 photocatalyst was synthesized by a ball milling method, according to the following procedure: Firstly, 5 g of TiO_2, six Φ 10 and twenty Φ 6 agate balls were added to the agate jar. After being ground for several minutes, La_2O_3 with the corresponding mass percentage of 0.6% and a small amount of deionized water were added and heated to 80 °C. Then, the hydrochloric acid with the volume ratio of 1:1 was slowly added into the above solution and stirred until the solid was dissolved completely. Then, the deionized water was added to the total volume of 10 mL. The speed of the ball mill was set to 500 r/min, and the ball milling time was 4 h. The ball-milled slurry was washed with water, centrifuged, dried, and ground to obtain the La^{3+}/TiO_2 photocatalyst.

2.4. Preparation of Film and Photocatalytic Experiments

The preparation process and photocatalysis experiment of the La^{3+}/TiO_2/PVC film are shown in Figure 1. All raw materials need to be vacuum dried. The doping content of the La^{3+}/TiO_2 photocatalyst in the film were as a mass percentage of 0.1, 0.5, 1, 1.5, and 2, respectively. Hence, 2 g of PVC and 15 g of organic solvent DMF were added separately, heated, and stirred for 1 h. The mixed solution was ultrasonicated for 10 min so that the photocatalyst could be better mixed with the polymer. At room temperature, the mixed solution was dropped on the automatic film scraping machine and run at constant speed to prepare a film with a thickness of 150 μm. The flat plate was removed from the automatic film scraping machine and immersed in deionized water to obtain a composite film. The composite film was placed in the XPA-System photochemical reactor for light irradiation. The light source was a 300 W medium-pressure UV lamp with main wavelength of 365 nm. and the distance between the light source and the sample was 20 cm. The sample was taken out every 5 h, and the total illumination time was 30 h. The sample was taken out for storage and performance testing. The weight loss calculation formula is presented in Equation (1):

$$Weightloss\ (\%) = W_0 - W_t/W_0 \times 100\% \quad (1)$$

where W_t is the weight of film at after illumination and W_0 is the initial weight of film.

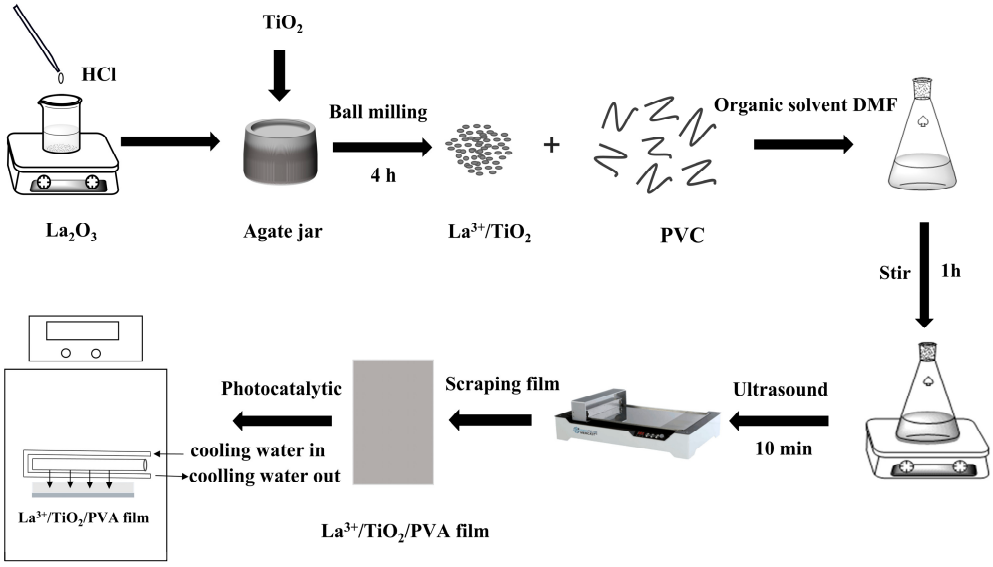


Figure 1. Preparation process of La^{3+}/TiO_2/PVC composite film by using La^{3+}/TiO_2 photocatalyst and the schematic diagram of the photodegradation equipment.

3. Results and Discussion

3.1. Characterization of La^{3+}/TiO_2 Photocatalyst

Figure 2A shows the XRD spectrum of La^{3+}/TiO_2 and raw TiO_2 after ball milling. Compared with TiO_2, the 3 mol% La^{3+}/TiO_2 still maintained the anatase crystal after doping, and no other peaks of rutile crystal was observed. This suggested that La^{3+} doped TiO_2 could inhibit the appearance of rutile crystal by ball milling method [22]. Moreover, no obvious characteristic peaks of the La^{3+} were found, possibly due the small content of La^{3+} doped into the TiO_2 lattice. Furthermore, the ionic radius of La^{3+} was larger than that of Ti^{4+}, so these doped ions might have difficulty in entering the TiO_2 lattice. The peak position of the (101) crystal plane in La^{3+}/TiO_2 appeared red-shifted to 25.4°, indicating that La^{3+} could be highly dispersed on the TiO_2 surface in a free state [23]. As shown in Figure 2B, the EDX spectra indicate that the sample was mainly formed of Ti, O, and La, suggesting that La^{3+} successfully doped to TiO_2. La^{3+} was dispersed on the surface of

TiO_2, and it had a squeezing effect on the TiO_2 lattice, resulting in more crystal defects and distortions, which had a certain effect on the TiO_2 crystal [24,25].

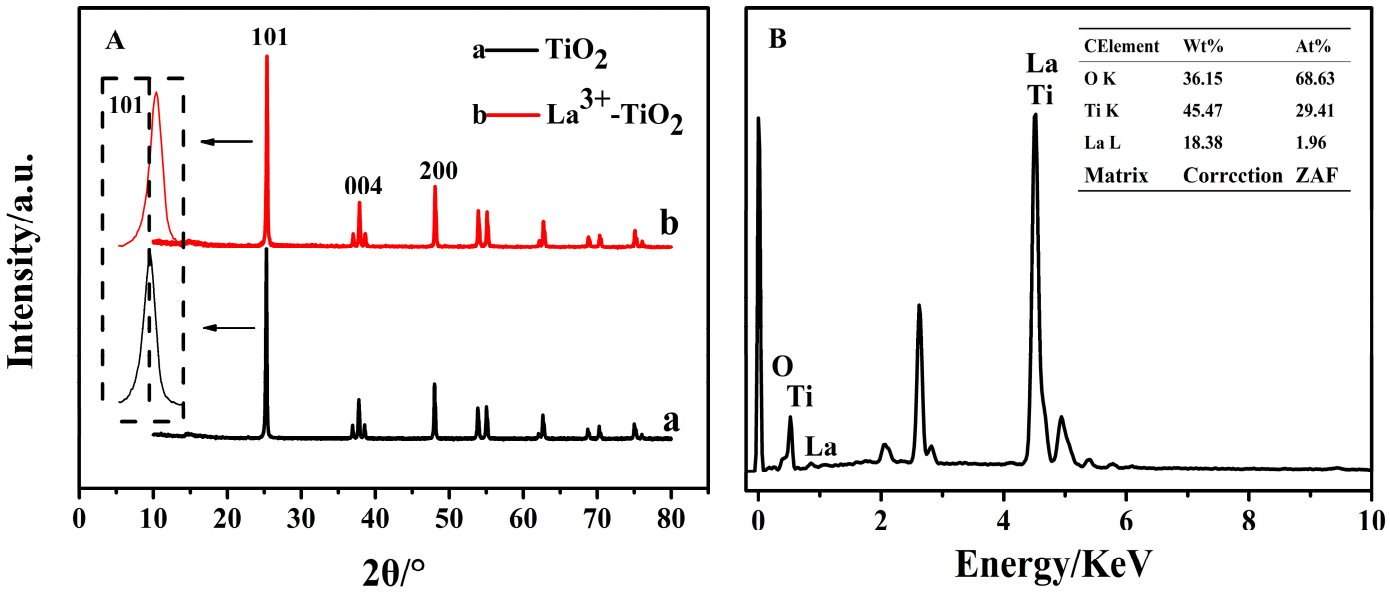


Figure 2. Characterization of the La^{3+}/TiO_2. (**A**) XRD pattern; (**B**) EDX spectra and component molar ratio.

Figure 3 shows the FT-IR spectrum of raw TiO_2 and 0.6 wt% La^{3+}/TiO_2. A strong characteristic peak between 2700 and 3600 cm^{-1} was attributed to -OH in the H_2O molecule, while the corresponding bending vibration peak appeared near 1630 cm^{-1} [26]. The characteristic peaks between approximately 500 and 900 cm^{-1} belonged to the anatase O-Ti-O bond [27]. After La^{3+} doping, the strong peaks of the defective -OH groups obviously weakened, as the OH groups on the surface of TiO_2 could be covalently bonded to La^{3+} [28]. A decrease in the characteristic peak of the anatase O-Ti-O bond was attributed to the covalent band between La^{3+} and TiO_2 particles, further indicating that La^{3+} was successfully doped to TiO_2.

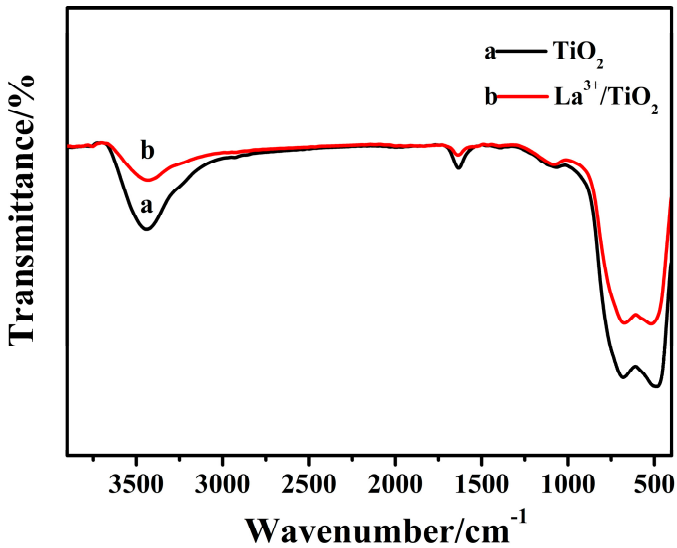


Figure 3. The FT-IR spectra of TiO_2 and La^{3+}/TiO_2.

Figure 4A shows the UV-visible absorption spectra of TiO_2 and La^{3+}/TiO_2. Compared with TiO_2, the UV absorption of La^{3+}/TiO_2 prepared by the ball milling method had little

change except a slight redshift. However, the absorption of La^{3+}/TiO_2 slightly enhanced in the visible region. The red shift of the absorption band was one of the important factors that made the sample have good photocatalytic performance under visible light. The reduced band gap energy of La^{3+}/TiO_2 could excite and produce more photo-generated electron-hole pairs, thus effectively improving the photocatalytic efficiency [29]. As shown in Figure 4B, the light absorption properties of PVC, TiO_2/PVC, La^{3+}/TiO_2/PVC composite films were also investigated. The PVC film had little absorption in both ultraviolet and visible region. The absorption of the TiO_2/PVC film significantly enhanced in the near ultraviolet region. The absorption band of La^{3+}/TiO_2/PVC appeared red-shifted and could absorb light energy in the visible region. The red shift was mainly because part of La^{3+} was embedded on TiO_2 to form defect energy levels, which reduced the energy level spacing during electron transition [30]. Therefore, it was of great significance to use La^{3+}/TiO_2 with the higher photocatalytic activity to enhance the degradation performance of PVC.

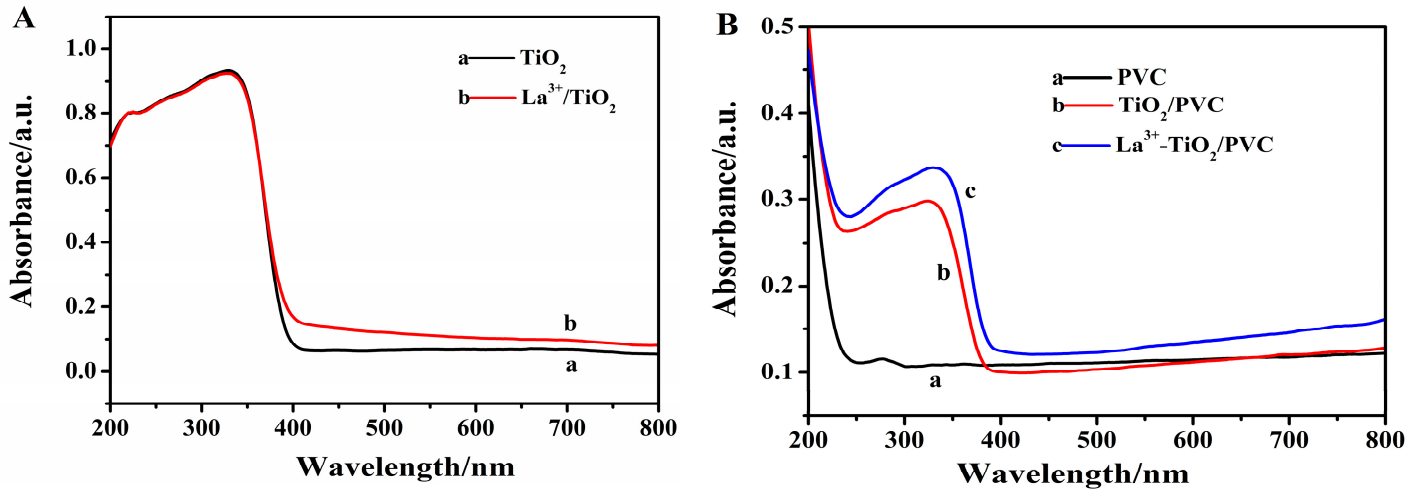


Figure 4. UV-visible absorption spectrum. (**A**) (a) TiO_2 (b) La^{3+}/TiO_2; (**B**) (a) Pure PVC sample, (b) TiO_2/PVC sample, (c) La^{3+}/TiO_2/PVC sample.

3.2. Photodegradation of La^{3+}/TiO_2/PVC

In order to obtain a film with the best degradation effect, La^{3+}/TiO_2 was mixed with PVC to make the composite films with different mass percentages, and the photodegradation rates of the above La^{3+}/TiO_2/PVC composite films were compared with those of PVC and TiO_2/PVC after irradiation (Figure 5). After light irradiation, the weight loss rate of the PVC was only 2.12%, while that of the TiO_2/PVC reached 8.94%. The accelerating of the degradation rate was due to the mixing of TiO_2 into PVC. As for the La^{3+}/TiO_2/PVC composite film, when the mass percentage of La^{3+}/TiO_2 was 1.5%, the weight loss rate of La^{3+}/TiO_2/PVC sample reached a maximum of 17.78%, which was eight times the degradation rate of PVC and two times the degradation rate of TiO_2/PVC. Obviously, the photocatalytic activity of La^{3+}/TiO_2/PVC film increased greatly. Rare earth La^{3+} modified TiO_2 could inhibit the recombination of photo-generated electrons and holes and accelerate the formation of active oxides [31]. Moreover, the ball milling method was beneficial to the uniform distribution of La^{3+} and suppressed the TiO_2 agglomeration. After repeated grinding, the TiO_2 particles could be made smaller and its surface area increased [32,33], which supplied more photocatalytic active sites and further accelerated the degradation rate of PVC.

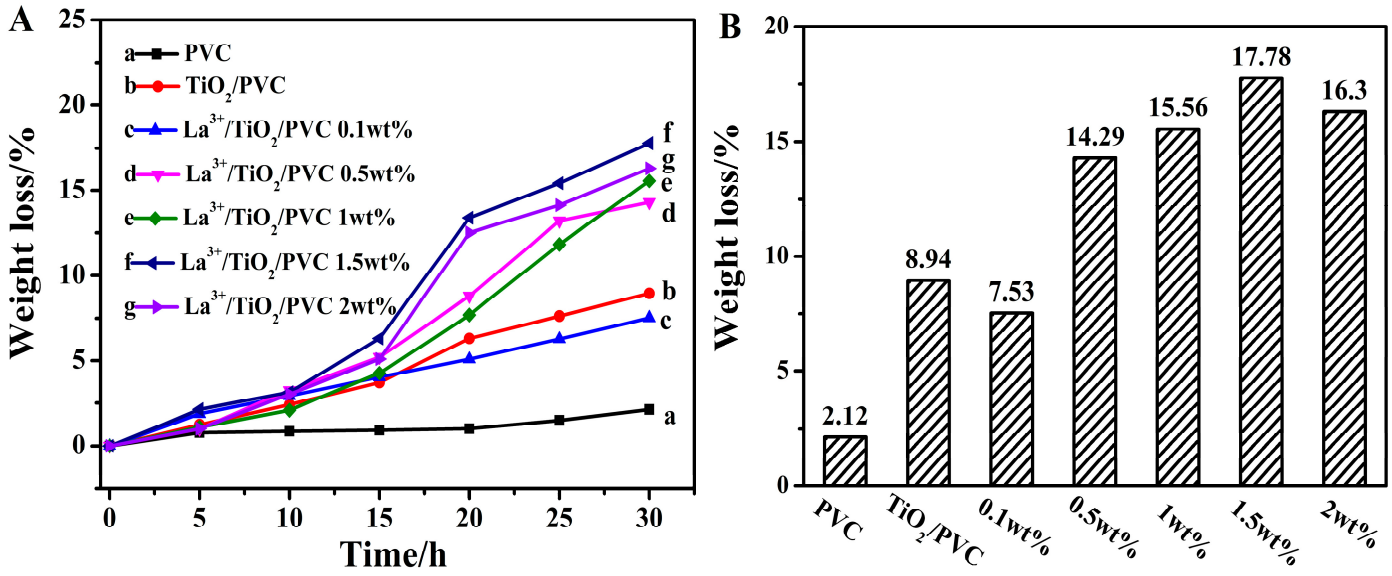


Figure 5. (**A**) Curves of weight loss of degradation process. (a) Pure PVC sample, (b) TiO_2/PVC sample, (c) La^{3+}/TiO_2/PVC (La^{3+}/TiO_2 0.1 wt%), (d) La^{3+}/TiO_2/PVC (0.5 wt%), (e) La^{3+}/TiO_2/PVC (1 wt%), (f) La^{3+}/TiO_2/PVC (1.5 wt%), (g) La^{3+}/TiO_2/PVC (2 wt%). (**B**) Maximum weight loss rate.

Figure 6A compares the FT-IR spectrum of pure PVC, TiO_2/PVC, La^{3+}/TiO_2/PVC samples after being UV irradiated for 30 h with that of the original samples. As shown in Table 1, The characteristic peaks of C-H for the original PVC film appeared at 2973 cm^{-1}, 2917 cm^{-1}, and 1427 cm^{-1} [34]. The characteristic peaks at 698 cm^{-1} and 624 cm^{-1} belonged to the C-Cl, and the characteristic peaks at 1097 cm^{-1} belonged to the C-C of the PVC film [35]. Moreover, characteristics peak of TiO_2 could be seen in the spectrum of TiO_2/PVC and La^{3+}/TiO_2/PVC samples. The stretching vibration peak at 478 cm^{-1} belonged to Ti-O-Ti [36]. Obviously, a new band of at 1720 cm^{-1} was assigned to the C = O structure after illumination. The intensity of the characteristic peak of the C = O structure of the La^{3+}/TiO_2/PVC film increased gradually after 0 h,10 h, 20 h, and 30 h of irradiation (Figure 6B), indicating that the film was degraded with the continuous irradiation of light source. Due to the fact that La^{3+}/TiO_2 produces active oxides under UV irradiation. O_2^- or OH free radicals attacked the PVC molecular chain, and O_2 also participated in the reaction to generate oxygen-containing groups and caused the photodegradation of PVC [37]. La^{3+} can effectively separate the hole-electron pair of TiO_2 to generate more free radicals to attack PVC, which can increase the degradation rate of plastics.

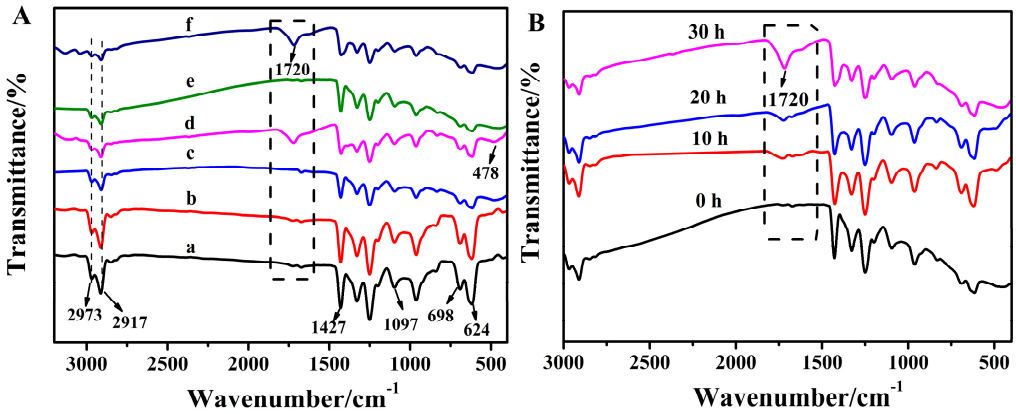


Figure 6. FT-IR spectra of polymer films. (**A**) (a) PVC before irradiation (b) PVC after irradiation, (c) TiO_2/PVC before irradiation (d) TiO_2/PVC after irradiation, (e) La^{3+}/TiO_2/PVC before irradiation (f) La^{3+}/TiO_2/PVC after irradiation. (**B**) La^{3+}/TiO_2/PVC after irradiation for 0 h, 10 h, 20 h, 30 h.

Table 1. The characteristic peak of infrared spectrum structure.

Serial Number	Wavenumber/cm^{-1}	Characteristic Peak
1	2973, 2917, 1427	C-H
2	698, 624	C-Cl
3	1097	C-C
4	478	Ti-O-Ti
5	1720	C=O

Figure 7 shows the XRD patterns of PVC, TiO_2/PVC, and La^{3+}/TiO_2/PVC films before and after UV irradiation. There was no obvious sharp characteristic diffraction peak of PVC, which clearly illustrated that PVC polymer was an amorphous structure, and the peak distribution was wide and low [38]. The characteristic diffraction peaks of TiO_2 appeared in the TiO_2/PVC film. After light illumination, the peaks of TiO_2/PVC and La^{3+}/TiO_2/PVC films disappeared at 13°~20°, while the pure PVC did not change. This was due to the destruction of the PVC structure in the photocatalyst/UV system. A new peak appeared at 32.5° in all composite films after light illumination, because several new small molecules appeared in the process of breaking PVC, which corresponded to the FT-IR spectrum.

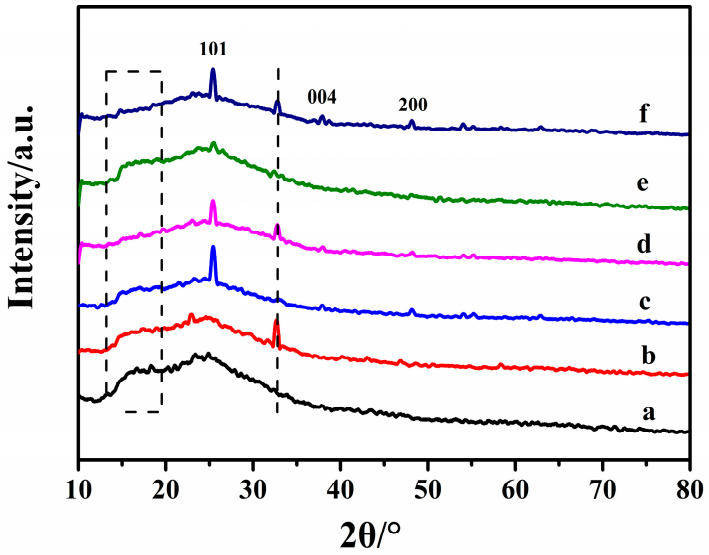


Figure 7. The XRD pattern for films. (**a**) PVC before irradiation (**b**) PVC after irradiation, (**c**) TiO_2/PVC before irradiation (**d**) TiO_2/PVC after irradiation, (**e**) La^{3+}/TiO_2/PVC before irradiation (**f**) La^{3+}/TiO_2/PVC after irradiation.

The surface structure of the film could be clearly observed by SEM. As shown in Figure 8, the surface of pure PVC, TiO_2/PVC and La^{3+}/TiO_2/PVC film had a certain size of hole before illumination. After UV irradiation, the size of the holes in PVC film increased slightly, while that in the TiO_2/PVC film significantly increased in terms of porosity and appeared to be crispy, indicating that a photo-oxidation reaction occurred on the film surface. The La^{3+}/TiO_2/PVC composite film could be seen to gradually undergo photooxidation after 10 h, 20 h, and 30 h UV exposure. Under 30 h illumination, the hole diameter increased to approximately 2–8 μm, and the La^{3+}/TiO_2 particles could be observed on the La^{3+}/TiO_2/PVC sample (Figure 8C4). As shown in the inset in Figure 8C4, the film appeared to fracture and the lanthanum ion-doped TiO_2 photocatalyst was observed at the place of the break, which indicated that the photo-oxidation was caused by the exposed La^{3+}/TiO_2. Therefore, the photodegradable film prepared by this method had certain application prospects for environmental friendliness.

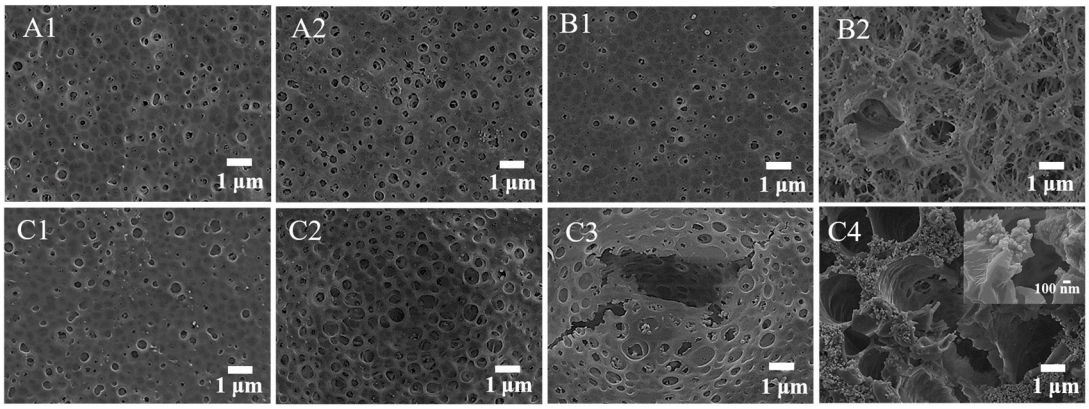


Figure 8. SEM images of films. (**A1**) PVC before irradiation, (**A2**) PVC after irradiation; (**B1**) TiO_2/PVC before irradiation, (**B2**) TiO_2/PVC after irradiation; (**C1**) La^{3+}/TiO_2/PVC before irradiation, La^{3+}/TiO_2/PVC after irradiation for (**C2**) 10 h, (**C3**) 20 h, (**C4**) 30 h.

3.3. The Performance Characterization of La^{3+}/TiO_2/PVC

One of the important reasons why the additive degradable plastics have not been widely used was the poor mechanical properties of plastics. Therefore, it is of great significance to study the tensile properties of the La^{3+}/TiO_2/PVC plastics. There were two important factors influencing the mechanical properties of materials: (1) the shape, orientation, and distribution of the additive, (2) the interaction between the additive and the matrix [39,40]. As shown in Table 2, after mixing PVC and TiO_2 or La^{3+}/TiO_2, the tensile strength and elongation of PVC decreased slightly. The slight decrease in mechanical properties might be due to the mixture of amorphous and crystalline TiO_2 in the PVC chain, which reduced the polymer interaction between chains [41]. However, the La^{3+}/TiO_2/PVC degradable was made by this method and belonged to an environment-friendly composite material.

Table 2. Mechanical properties of these kinds of different films.

Sample	Thickness (mm)	Tensile Strength (MPa)	Elongation at Break (%)
PVC	0.12 ± 0.01	2.10 ± 0.20	31 ± 0.08
TiO_2/PVC (TiO_2 1 wt%)	0.11 ± 0.01	1.70 ± 0.10	26 ± 0.10
La^{3+}/TiO_2/PVC (La^{3+}/TiO_2 1.5 wt%)	0.13 ± 0.01	1.71 ± 0.17	31 ± 0.04

The thermal degradation of PVC was mainly divided into two stages (Figure 9). The first stage was the removal of HCl from PVC, where most of the degradation products in the second stage were cyclic compounds [42]. Compared with pure PVC film, the initial degradation temperature of PVC composite films had no obvious change. However, the overall degradation temperature shifted to a higher temperature, and the thermal stability of PVC composite film was improved. The mass of films did not decrease around 100 °C, indicating that the films did not contain water molecules. At 800 °C, the PVC achieved complete thermal degradation.

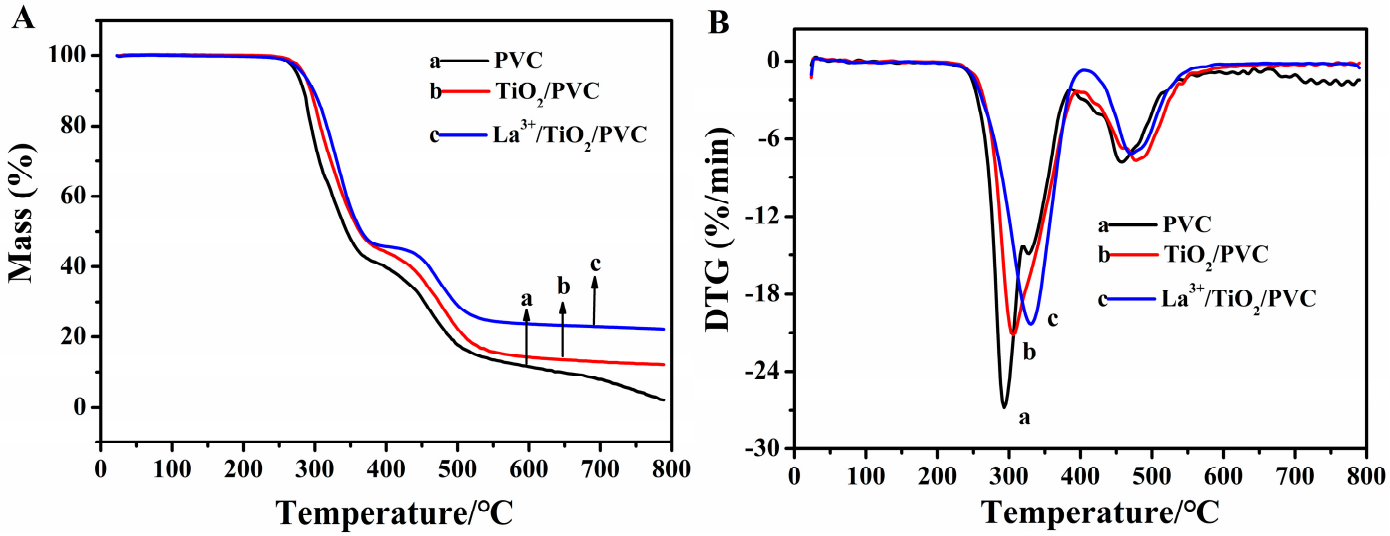


Figure 9. (**A**) TG and (**B**) DTG curves of three kinds of films.

3.4. Mechanism Discussion

La^{3+} doping modified TiO_2 has important significance for the increase of the TiO_2 photocatalytic activity. The reaction mechanism is shown in Figure 10. La^{3+} doped TiO_2 could inhibit the growth of TiO_2 grains and cause lattice distortion by the ball milling process. The grain refinement increased the specific surface area of TiO_2, provided more photocatalytic active sites, and improved the photocatalytic activity of TiO_2. When La ions were doped into the TiO_2 lattice, La^{3+} could capture photo-generated electrons to form La^{2+} (Formula (2)), and La^{2+} could easily form superoxide radicals with O_2 (Formula (3)), effectively inhibiting photo-generated carrier recombination (Formula (4)). Under the sufficient light energy, the valence band electrons of TiO_2 were excited to the conduction band. The outer electronic structure of the La element contained only one electron in the d orbit and the completely empty f orbit. Therefore, the empty orbits provided the transfer orbits for electrons (Formula (5)), which could be used as shallow traps to capture the photogenerated electrons, as well as facilitate the separation of photogenerated electron hole pairs. OH was formed by the reaction of photogenerated holes with H_2O on TiO_2 (Formula (6)). The photogenerated electrons reacted with O_2 to produce O_2^- and OH (Formulas (7)–(10)) [43]. During the photodegradation process of high-molecular polymers, the PVC molecular chains were attacked by O_2^- and OH to generate a free radical chain. According to the chemical bond energies of C-Cl, C-C, and C-H, 328 kJ/mol, 348 kJ/mol, and 413 kJ/mol, respectively, C-Cl was more easily destroyed by the free radicals generated under UV light (Formulas (11) and (12)). Then, the free radical chain continued to react with O_2 to form oxygen-containing compounds, which were decomposed into small molecules under the action of UV light, and finally completely mineralized (Formulas (13) and (14)). Moreover, La^{3+} doping modified TiO_2 could inhibit the growth of TiO_2 grains and cause lattice distortion by ball milling process. The grain refinement increased the specific surface area of TiO_2, supplying more photocatalytic active sites and improving the photocatalytic activity of TiO_2. The La^{3+} doping would also change the band gap of TiO_2, so that La^{3+}/TiO_2 had absorption in the visible region [44]. Therefore, it is of great significance to use La^{3+}/TiO_2 with the higher photocatalytic activity to enhance the degradation performance of PVC.

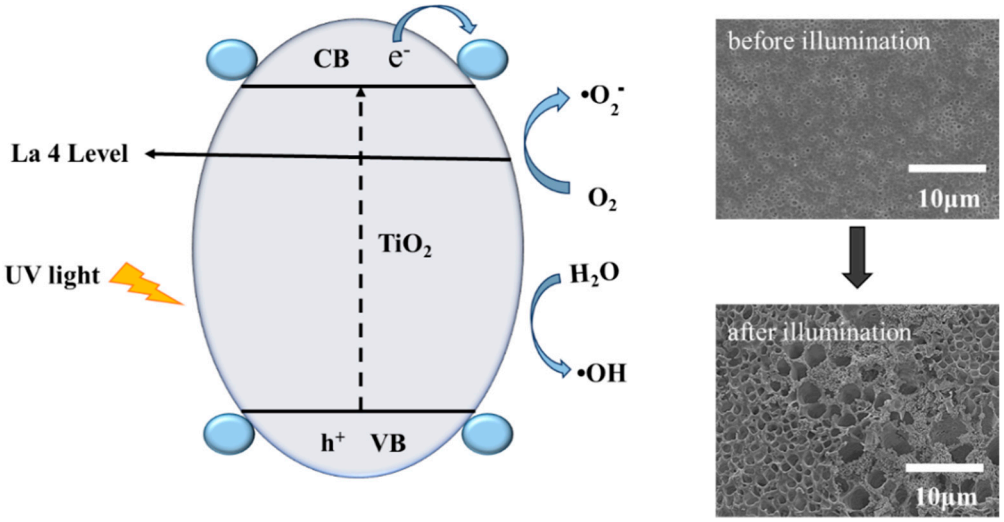


Figure 10. Photocatalytic degradation mechanism of La^{3+}/TiO_2/PVC.

$$La^{3+} + e^- \rightarrow La^{2+} \quad (2)$$

$$La^{2+} + O_2 \rightarrow La^{3+} + \bullet O_2^- \quad (3)$$

$$2\bullet O_2^- + 2H^+ + e^- \rightarrow \bullet O_2H + OH^- + O_2 \quad (4)$$

$$TiO_2 + h\nu \rightarrow TiO_2\ (e^- + h^+) \quad (5)$$

$$h^+ + H_2O \rightarrow \bullet OH \quad (6)$$

$$e^- + O_2 \rightarrow \bullet O_2^- \quad (7)$$

$$\bullet O_2^- + H_2O \rightarrow \bullet O_2H + OH^- \quad (8)$$

$$2\bullet O_2H \rightarrow H_2O_2 + O_2 \quad (9)$$

$$H_2O_2 + h\nu \rightarrow 2\bullet OH \quad (10)$$

$$-(CH_2CHClCH_2CHCl)- + \cdot OH + h\nu \rightarrow -(CHCHCH_2CH)- + H_2O + 2\cdot Cl \quad (11)$$

$$-CH\cdot CHCH_2CH\cdot CH_2- + 2\cdot Cl \rightarrow -CHCH=CHCH=CH- + 2\,HCl \quad (12)$$

$$-CH=CH\text{-}CH_2- + {}^1O_2 \rightarrow -(HOO)CH\text{-}CH=CH- \quad (13)$$

$$-(CHCH=CHCH)- + O_2 \rightarrow \rightarrow CO_2 + H_2O \quad (14)$$

4. Conclusions

An La^{3+}/TiO_2 photocatalyst was successfully prepared and characterized by the ball milling method. The characterization results showed that La^{3+} successfully doped modified TiO_2. La^{3+} was dispersed on the surface of TiO_2, increasing the surface oxygen vacancies and lattice distortion. Compared with TiO_2, the La^{3+}/TiO_2 photocatalyst showed higher photocatalytic activity. La^{3+}/TiO_2 was applied to photocatalytic degradation of PVC plastic. After 30 h of UV light irradiation, the weight loss rate of the PVC and TiO_2/PVC were 2.12% and 8.94%, respectively, while that of the La^{3+}/TiO_2/PVC (La^{3+}/TiO_2 1.5 wt%) reached 17.78%, which was eight times the degradation rate of PVC and two times the degradation rate of TiO_2/PVC. The La^{3+}/TiO_2/PVC composite film showed higher photodegradability. After illumination, the FT-IR spectrum showed a new peak at 1720 cm^{-1}, which belonged to C = O, and the XRD patterns showed a new peak at 32.5°. The surface pore size of the La^{3+}/TiO_2/PVC sample increased to 2~8 μm. These results indicated that the La^{3+}/TiO_2/PVC film had photodegradability. Predictably, La^{3+}/TiO_2/PVC has a good application prospect, and it is an environment-friendly composite material.

Author Contributions: Conceptualization, Z.S. and T.S.; methodology, D.Z.; software, Y.Z.; validation, C.L. and J.L.; formal analysis, B.L.; investigation, Y.Z.; resources, Z.S.; data curation, Y.Z.; writing—original draft preparation, Y.Z.; writing—review and editing, T.S.; supervision, T.S.; project administration, Z.S.; funding acquisition, Z.S. All authors have read and agreed to the published version of the manuscript.

Funding: This research received no external funding.

Institutional Review Board Statement: Not applicable.

Informed Consent Statement: Not applicable.

Data Availability Statement: Not applicable.

Acknowledgments: This research was supported by the National Natural Science Foundation of China (Grant No. 22168017), the Hainan Provincial Natural Science Foundation of China (2019RC183, 2019RC187, 420QN259, 222CXTD513 and 420QN251), and the Scientific Research Project of Higher Education of Hainan Province (HNKY 2020–2026), the Graduate Innovative Research Project of Hainan Province (Qhyb2022-104).

Conflicts of Interest: The authors declare no conflict of interest.

References

1. Li, M.; Xia, J.; Ding, H.; Ding, C.; Wang, M.; Li, S. Optimal design, characterization, and thermal stability of bio-based ca/na/zn composite stabilizer derived from myrcene for poly(vinyl chloride). *Polym. Degrad. Stabil.* **2017**, *139*, 117–129. [CrossRef]
2. Jia, P.; Hu, L.; Shang, Q.; Wang, R.; Zhang, M.; Zhou, Y. Self-plasticization of pvc materials via chemical modification of mannich base of cardanol butyl ether. *ACS Sustain. Chem. Eng.* **2017**, *5*, 6665–6673. [CrossRef]
3. Iwata, T. Biodegradable and bio-based polymers: Future prospects of eco-friendly plastics. *Angewandte. Chem.* **2015**, *46*, 3210–3215. [CrossRef]
4. Borrelle, S.B.; Rochman, C.M.; Liboiron, M.; Bond, A.L.; Lusher, A.; Bradshaw, H.; Provencher, J.F. Opinion: Why we need an international agreement on marine plastic pollution. *Proc. Natl. Acad. Sci. USA* **2017**, *114*, 9994–9997. [CrossRef] [PubMed]
5. Canopoli, L.; Fidalgo, B.; Coulon, F.; Wagland, S.T. Physico-chemical properties of excavated plastic from landfill mining and current recycling routes. *Waste Manag.* **2018**, *76*, 55–67. [CrossRef] [PubMed]
6. Das, P.; Roy, A.; Chakrabarti, S.J. Photocatalytic degradation of the nanocomposite film comprising polyvinyl chloride (PVC) and sonochemically synthesized iron-doped zinc oxide: A comparative study of performances between sunlight and uv radiation. *Polym. Environ.* **2017**, *25*, 1231–1241. [CrossRef]
7. Najafi, V.; Ahmadi, E.; Ziaee, F.; Omidian, H.; Sedaghat, H. Polyaniline-modified TiO_2, a highly effective photo-catalyst for solid-phase photocatalytic degradation of PVC. *J. Polym. Environ.* **2019**, *27*, 784–793. [CrossRef]
8. Zhang, Y.; Sun, T.; Zhang, D.; Shi, Z.; Zhang, X.; Li, C.; Wang, L.; Song, J.; Lin, Q. Enhanced photodegradability of PVC plastics film by codoping nano-graphite and TiO_2. *Polym. Degrad. Stabil.* **2020**, *181*, 109332. [CrossRef]
9. Cho, S.; Choi, W. Solid-phase photocatalytic degradation of PVC–TiO_2 polymer composites. *J. Photoch. Photobio. A* **2001**, *143*, 221–228. [CrossRef]
10. Dastgeer, G.; Afzal, A.M.; Jaffery, S.H.A.; Imran, M.; Assiri, M.A.; Nisar, S. Gate modulation of the spin current in graphene/WSe_2 van der Waals heterostructure at room temperature. *J. Alloys Compd.* **2022**, *919*, 919. [CrossRef]
11. Sun, T.; Zhao, Z.; Liang, Z.; Liu, J.; Shi, W.; Cui, F. Efficient removal of arsenite through photocatalytic oxidation and adsorption by ZrO_2-Fe_3O_4 magnetic nanoparticles. *Appl. Surf. Sci.* **2017**, *416*, 656–665. [CrossRef]
12. Tsebriienko, T.; Popov, A.I. Effect of poly (titanium oxide) on the viscoelastic and thermophysical properties of interpenetrating polymer networks. *Crystals* **2021**, *11*, 794. [CrossRef]
13. Serga, V.; Burve, R.; Krumina, A.; Romanova, M.; Kotomin, E.A.; Popov, A.I. Extraction–pyrolytic method for TiO_2 polymorphs production. *Crystals* **2021**, *11*, 431. [CrossRef]
14. Serga, V.; Burve, R.; Krumina, A.; Pankratova, V.; Popov, A.; Pankratov, V. Study of phase composition, photocatalytic activity, and photoluminescence of TiO_2 with Eu additive produced by the extraction-pyrolytic method. *J. Mater. Res. Technol.* **2021**, *13*, 2350–2360. [CrossRef]
15. Cerrato, E.; Gaggero, E.; Calza, P.; Paganini, M.C. The role of Cerium, Europium and Erbium doped TiO_2 photocatalysts in water treatment: A mini-review. *Adv. Chem. Eng.* **2022**, *10*, 100268. [CrossRef]
16. Soundarya, T.L.; Jayalakshmi, T.; Alsaiari, M.A.; Jalalah, M.; Abate, A.; Alharthi, F.A.; Ahmad, N.; Nagaraju, G. Ionic liquid-aided synthesis of anatase TiO_2 nanoparticles: Photocatalytic water splitting and electrochemical applications. *Crystals* **2022**, *12*, 1133. [CrossRef]
17. Aksimentyeva, O.I.; Savchyn, V.P.; Dyakonov, V.P.; Piechota, S.; Horbenko, Y.Y.; Opainych, I.Y.; Demchenko, P.Y.; Popov, A.; Szymczak, H. Modification of polymer-magnetic nanoparticles by luminescent and conducting substances. *Mol. Cryst. Liq. Cryst.* **2014**, *590*, 35–42. [CrossRef]
18. Song, L.; Zhao, X.; Cao, L.; Moon, J.W.; Gu, B.; Wang, W. Synthesis of rare earth doped TiO_2 nanorods as photocatalysts for lignin degradation. *Nanoscale* **2015**, *7*, 16695–16703. [CrossRef] [PubMed]

19. Reszczyńska, J.; Grzyb, T.; Sobczak, J.W.; Lisowski, W.; Gazda, M.; Ohtani, B.; Zaleska, A. Visible light activity of rare earth metal doped (Er^{3+}, Yb^{3+} or Er^{3+}/Yb^{3+}) titania photocatalysts. *Appl. Catal. B-Environ.* **2015**, *163*, 40–49. [CrossRef]
20. Setiawati, E.; Kawano, K. Stabilization of anatase phase in the rare earth; Eu and Sm ion doped nanoparticle TiO_2. *J. Alloys Compd.* **2008**, *451*, 293–296. [CrossRef]
21. Fang, X.L.; Chen, X.H.; Zhu, Z.S. Optical and photocatalytic properties of Er^{3+} and/or Yb^{3+} doped TiO_2 photocatalysts. *J. Mater. Sci-Mater. REl.* **2017**, *28*, 474–479. [CrossRef]
22. Soares, O.S.G.P.; Rocha, R.P.; Gonçalves, A.G.; Figueiredo, J.L.; Órfão, J.J.M.; Pereira, M.F.R. Highly active N-doped carbon nanotubes prepared by an easy ball milling method for advanced oxidation processes. *Appl. Catal. B-Environ.* **2016**, *192*, 296–303. [CrossRef]
23. Jiang, H.; Liu, Y.; Li, J.; Wang, H. Synergetic effects of lanthanum, nitrogen and phosphorus tri-doping on visible-light photoactivity of TiO_2 fabricated by microwave-hydrothermal process. *J. Rare. Earth* **2016**, *34*, 604–613. [CrossRef]
24. Wu, D.; Li, C.; Kong, Q.; Shi, Z.; Zhang, D.; Wang, L.; Han, L.; Zhang, X.; Lin, Q. Photocatalytic activity of Lu^{3+}/TiO_2 prepared by ball milling method. *J. Rare. Earth* **2018**, *36*, 819–825. [CrossRef]
25. Wu, D.; Li, C.; Zhang, D.; Wang, L.; Zhang, X.; Shi, Z.; Lin, Q. Photocatalytic improvement of Y^{3+} modified TiO_2 prepared by a ball milling method and application in shrimp wastewater treatment. *RSC Adv.* **2019**, *9*, 14609–14620. [CrossRef]
26. Shojaie, A.F.; Loghmani, M.H. La^{3+} and Zr^{4+} Co-doped anatase nano TiO_2 by sol-microwave method. *Chem. Eng. J.* **2010**, *157*, 263–269. [CrossRef]
27. Dvoranováa, D.; Brezováa, V.; Mazúra, M.; Malatib, M.A. Investigations of metal-doped titanium dioxide photocatalysts. *Appl. Catal. B-Environ.* **2002**, *37*, 91–105. [CrossRef]
28. Kumaresan, L.; Prabhu, A.; Palanichamy, M.; Arumugam, E.; Murugesan, V. Synthesis and characterization of Zr^{4+}, La^{3+} and Ce^{3+} doped mesoporous TiO_2: Evaluation of their photocatalytic activity. *J. Hazard. Mater.* **2011**, *186*, 1183–1192. [CrossRef]
29. Liu, R.; Ren, Y.; Wang, J.; Wang, Y.; Jia, J.; Zhao, G. Preparation of Nb-doped TiO_2 films by sol-gel method and their dual-band electrochromic properties. *Ceram. Int.* **2021**, *47*, 31834–31842. [CrossRef]
30. Xu, Z.; Jiang, Y.; Gui, C. Based on the study on preparation and properties of Co (II) and La^{3+}-doped TiO_2 electrochromic film. *Integr. Ferroelectr.* **2020**, *209*, 58–67.
31. Jia, Z.; La, L.B.T.; Zhang, W.C.; Liang, S.X.; Jiang, B.; Xie, S.K.; Habibi, D.; Zhang, L.C. Strong enhancement on dye photocatalytic degradation by ball-milled TiO_2: A study of cationic and anionic dyes. *J. Mater. Sci. Technol.* **2017**, *33*, 856–863. [CrossRef]
32. Miao, J.; Zhang, R.; Zhang, L. Photocatalytic degradations of three dyes with different chemical structures using ball-milled TiO_2. *Mater. Res. Bull.* **2018**, *97*, 109–114. [CrossRef]
33. Cong, Y.; Tian, B.; Zhang, J. Improving the thermal stability and photocatalytic activity of nanosized titanium dioxide via La^{3+} and N co-doping. *J. Appl. Catal. B-Environ.* **2011**, *101*, 376–381. [CrossRef]
34. Liu, G.; Zhu, D.; Zhou, W.; Liao, S.; Cui, J.; Wu, K.; Hamilton, D. Solid-phase photocatalytic degradation of polystyrene plastic with goethite modified by boron under uv–vis light irradiation. *Appl. Surf. Sci.* **2010**, *256*, 2546–2551. [CrossRef]
35. Mallakpour, S.; Shamsaddinimotlagh, S. Ultrasonic-promoted rapid preparation of PVC/TiO_2-BSA nanocomposites: Characterization and photocatalytic degradation of methylene blue. *Ultrason. Sonochem.* **2018**, *41*, 361–374. [CrossRef]
36. Zhang, L.; Chen, L.; Wan, H.; Chen, J.; Zhou, H. Synthesis and tribological properties of stearic acid-modified anatase (TiO_2) nanoparticles. *Tribol. Lett.* **2011**, *41*, 409–416.
37. Chakrabarti, S.; Chaudhuri, B.; Bhattacharjee, S.; Das, P.; Dutta, B.K. degradation mechanism and kinetic model for photocatalytic oxidation of PVC–ZnO composite film in presence of a sensitizing dye and uv radiation. *J. Hazard. Mater.* **2008**, *154*, 230–236. [CrossRef]
38. Sagar, R.; Gaur, M.S.; Rogachev, A.A. Piezoelectric and pyroelectric properties of ceramic nanoparticles-based nanostructured PVDF/PVC blend nanocomposites. *J. Therm. Anal. Calorim.* **2021**, *146*, 645–655. [CrossRef]
39. Uddin, M.F.; Sun, C.T. Strength of unidirectional glass/epoxy composite with silica nanoparticle-enhanced matrix. compos. *Compos. Sci. Technol.* **2008**, *68*, 1637–1643. [CrossRef]
40. Mallakpour, S.; Abdolmaleki, A.; Tabebordbar, H. Production of PVC/α-MnO_2-KH550 manocomposite films: Morphology, thermal, mechanical and pb (II) adsorption properties. *Eur. Polym. J.* **2016**, *78*, 141–152. [CrossRef]
41. Roy, S.; Ryan, J.; Webster, S.; Nepal, D. A review of in situ mechanical characterization of polymer nanocomposites: Prospect and challenges. *Appl. Mech. Rev.* **2017**, *69*, 050802. [CrossRef]
42. Zhang, Y.; Shi, Z.; Sun, T.; Zhang, D.; Zhang, X.; Lin, X.; Li, C.; Wang, L.; Song, J.; Lin, Q. The preparation of a novel eco-friendly methylene blue/TiO_2/PVC composite film and its photodegradability. Polym-Plast. *Technol. Mat.* **2020**, *60*, 358–368.
43. Zan, L.; Tian, L.; Li, Z.; Peng, Z. A New polystyrene–TiO_2, nanocomposite film and its photocatalytic degradation. *Appl. Catal. A-Gen.* **2004**, *264*, 237–242. [CrossRef]
44. Rostami, M. Construction of La-doped TiO_2@ La-doped ZnO–B-doped reduced graphene oxide ternary nanocomposites for improved visible light photocatalytic activity. *RSC Adv.* **2017**, *7*, 43424–43431. [CrossRef]

Disclaimer/Publisher's Note: The statements, opinions and data contained in all publications are solely those of the individual author(s) and contributor(s) and not of MDPI and/or the editor(s). MDPI and/or the editor(s) disclaim responsibility for any injury to people or property resulting from any ideas, methods, instructions or products referred to in the content.